Chloride cotransporter KCC2 is essential for GABAergic inhibition in the SCN.

A.H.O. Olde Engberink[1], J.H. Meijer[1], S. Michel[1]*

[1]*Department of Cellular and Chemical Biology, Laboratory for Neurophysiology, Leiden University Medical Center, Einthovenweg 20, 2333 ZC, Leiden, the Netherlands.*

*corresponding author
Stephan Michel

S.H.Michel@lumc.nl

Postal address:
LUMC
Postzone S5-P
Postbus 9600
2300 RC Leiden
The Netherlands

Abstract

One of the principal neurotransmitters of the central nervous system is GABA. In the adult brain, GABA is predominantly inhibitory, but there is growing evidence indicating that GABA can shift to excitatory action depending on environmental conditions. In the mammalian central circadian clock of the suprachiasmatic nucleus (SCN) GABAergic activity shifts from inhibition to excitation when animals are exposed to long day photoperiod. The polarity of the GABAergic response (inhibitory versus excitatory) depends on the GABA equilibrium potential determined by the intracellular Cl^- concentration ($[Cl^-]_i$). Chloride homeostasis can be regulated by Cl^- cotransporters like NKCC1 and KCC2 in the membrane, but the mechanisms for maintaining $[Cl^-]_i$ are still under debate. This study investigates the role of KCC2 on GABA-induced Ca^{2+} transients in SCN neurons from mice exposed to different photoperiods. We show for the first time that blocking KCC2 with the newly developed blocker ML077 can cause a shift in the polarity of the GABAergic response. This will increase the amount of excitatory responses in SCN neurons and thus cause a shift in excitatory/inhibitory ratio. These results indicate that KCC2 is an essential component in regulating $[Cl^-]_i$ and the equilibrium potential of Cl^- and thereby determining the sign of the GABAergic response. Moreover, our data suggest a role for the Cl^- cotransporters in the switch from inhibition to excitation observed under long day photoperiod.

Keywords: GABA; KCC2; ML077; excitation/inhibition ratio; circadian; calcium

1. Introduction

The balance between neuronal inhibition and excitation is critical for proper brain functioning (Buzsaki et al., 2007; Haider et al., 2006). Accordingly, an imbalance is implicated in several neurological disorders, like epilepsy and autism (Marín, 2012; Nelson and Valakh, 2015; Sgadò et al., 2011). One of the important factors for keeping this balance is γ-Aminobutyric acid (GABA), known as the major inhibitory neurotransmitter in the central nervous system (Costa, 1998; Sivilotti and Nistri, 1991). In the developing brain, however, GABA can act as an excitatory neurotransmitter (Ben-Ari, 2002), and even in the mature brain, the phenomenon of GABAergic depolarization has recently been recognized and characterized in multiple areas (Chung, 2012). One of these brain areas is the mammalian central circadian clock, located in the suprachiasmatic nucleus (SCN) of the anterior hypothalamus (Choi et al., 2008; De Jeu and Pennartz, 2002; Wagner et al., 1997). GABA is the prevalent neurotransmitter in the SCN and involved in synchronization within the neuronal network and in processing photic as well as non-photic entrainment (Albers et al., 2017). While exogenous applied GABA causes an inhibitory effect on the firing rate in many SCN neurons, it has a distinct excitatory effect on a subset of neurons in the SCN. The excitation is typically found in the neurons of the dorsal part of the SCN and is especially present during the night (Choi et al., 2008). Interestingly, exposure to long day photoperiod changes the GABAergic excitation/inhibition ratio (E/I ratio) in SCN neurons towards more excitation compared to short day photoperiod (Farajnia et al., 2014). This demonstrates that GABAergic excitation can have a physiological function in the SCN of the mature brain, and that its effect is plastic, i.e. under the control of environmental conditions.

The major ion that passes through the $GABA_A$ receptor is chloride (Cl^-) (Macdonald and Olsen, 1994). The concentration gradient of Cl^- (the difference between internal and external concentrations) determines the equilibrium potential of chloride (E_{Cl}). Depending on the relationship between the E_{Cl} and the membrane potential (V_m), GABA acts either excitatory or inhibitory when binding to its receptor (Ben-Ari, 2002; Kaila, 1994).

It has generally been assumed that cation-chloride-cotransporters (CCCs) play a crucial role in maintaining the intracellular chloride concentration ($[Cl^-]_i$). In neurons, mainly two types of CCCs regulate $[Cl^-]_i$; the Na^+-K^+-$2Cl^-$ cotransporter 1 (NKCC1) and the K^+-Cl^- cotransporter 2 (KCC2), which carry Cl^- in and out of the cell, respectively (Blaesse et al., 2009; Deeb et al., 2011; Gamba, 2005). Glykys et al. recently challenged this view by showing that immobile negative charges near the extracellular surface of the cell membrane and cytoplasmic impermeant anions may also play a prominent role in determining $[Cl^-]_i$ (Glykys et al., 2014a).

Investigating the mechanism of $[Cl^-]_i$ regulation requires specific blockers for CCCs and a recent study using an improved KCC2 antagonist suggests a primary role of KCC2 in $[Cl^-]_i$ of SCN neurons (Klett and Allen, 2017). We used a recently developed and highly selective KCC2 antagonist; VU0255011; also known as ML077, which has over a hundredfold higher specificity for KCC2 over NKCC1 (Delpire et al., 2009; Lindsley et al., 2010). With this pharmacological tool, we were able to investigate the role of KCC2 in the GABAergic response. Here, we show that blocking KCC2 with ML077 can cause a shift in the polarity of the GABAergic response by inducing excitatory responses in previously inhibitory responding neurons. These results indicate that KCC2 is an essential component in regulating $[Cl^-]_i$ and the E_{Cl}, thereby determining the sign of the GABAergic response.

2. Materials and methods

2.1 Animals

Male C57BL/6 mice (Envigo, Horst, the Netherlands; 8–10 wk. old; n = 35) were housed in a climate controlled environment (21˚C, 40-50% humidity) on an equinoctial photoperiod of 12h light-dark (12:12; LD12:12), a long photoperiod (LP; LD16:8), or a short photoperiod (SP; LD8:16). Food and water were available ad libitum. Before recordings, the mice were exposed to their respective photoperiod for a minimum of 30 days to ensure entrainment to the given light schedule. Experiments were performed within a 4-h interval centered around the middle of the light-phase of the photoperiod. All animal experiments were performed in accordance with the regulations of the Dutch law on animal welfare, and the institutional ethics committee for animal procedures of the Leiden University Medical Center (Leiden, The Netherlands) approved the protocol.

2.2 Slice preparation

After decapitation, brains were quickly removed and placed into modified ice-cold artificial cerebrospinal fluid (ACSF), containing (in mM): NaCl 116.4, KCl 5.4, NaH_2PO_4 1.0, $MgSO_4$ 0.8, $CaCl_2$ 1, $MgCl_2$ 4, $NaHCO_3$ 23.8, glucose 15.1, and 5 mg/L gentamycine (Sigma Aldrich, Munich, Germany) and saturated with 95% O_2 – 5% CO_2. Coronal hypothalamic slices containing the SCN (250 µm) were cut using a vibratome (VT 1000S, Leica Microsystems, Wetzlar, Germany) and sequentially maintained in regular, oxygenated ACSF ($CaCl_2$ increased to 2 mM and without $MgCl_2$). The slices were incubated in a water bath (37˚C) for 30 minutes and were then maintained at room temperature until the start of the recordings.

2.3 Ca^{2+} imaging

Neurons in brain slices were bulk-loaded with the ratiometric, membrane permeable Ca^{2+} indicator dye fura-2-acetoxymethyl ester (Fura-2-AM) as described previously (Michel et al., 2013). Briefly, the slices were submerged into a mix of ACSF containing 7 µM Fura-2-AM for 10 minutes at 37˚C. The

slices were then rinsed four times with fresh ACSF before being transferred to a recording chamber (RC-26G, Warner Instruments, Hamden, CT, USA) mounted on the fixed stage of an upright fluorescence microscope (Axioskop 2-FS Plus, Carl Zeiss Microimaging, Oberkochen, Germany) and constantly perfused with oxygenated ACSF (2.5 mL/min) at room temperature. The indicator dye was excited alternatively at wavelengths of 340 and 380 nm by means of a monochromator (Polychrome V, TILL Photonics; now FEI Munich GmbH, Munich, Germany). Emitted light (505 nm) was detected by a cooled CCD camera (Sensicam, TILL Photonics; now FEI Munich GmbH, Munich, Germany), and images were acquired at 2 second intervals (Fig 1). Using an eight-channel pressurized focal application system (ALA-VM8, ALA scientific instruments, NY, USA) GABA (200 µM, 15 s) was applied locally and neuronal responses were recorded as Ca^{2+} transients. After two GABA pulses, which were separated by 1 minute baseline recording, ACSF containing elevated levels of K^+ (20 mM, 15 s) was applied to identify healthy, responding neurons. Cells with at least 10% increase in $[Ca^{2+}]_i$ in response to high levels of K^+ were considered as healthy cells. This protocol was repeated after 10 min incubation with either the drug ML077 (diluted in ACSF, 10 µM from 28 mM DMSO stock) or DMSO (diluted in ACSF, 4 ppm) via bath application (ML077: LP: n = 557 cells from eight animals; SP: n = 387 cells from eight animals; 12:12: n = 499 cells from eight animals. DMSO: LP: n = 319 cells from four animals; SP: n = 149 cells from three animals; 12:12: n = 248 cells from four animals). Both experiments and analysis were accomplished using imaging software (TILLvision, TILL Photonics; now FEI Munich GmbH, Munich, Germany). Single-wavelength images were background subtracted, and ratio images (340/380) were generated. Region of interest-defined cells and mean ratio values were determined, from which the intracellular Ca^{2+} concentration was calculated.

2.4 Chemicals

GABA, DMSO and all salts were purchased from Sigma-Aldrich. The first badge of ML077 was generously provided by Dr. Craig Lindsley (Vanderbilt University, Nashville, TN, USA) and thereafter

purchased from AOBIOUS (Gloucester, MA, USA). Fura-2-AM was purchased from TEFlabs (Austin, TX, USA).

2.5 Data analysis and statistics

Neuronal Ca^{2+} responses were analyzed using IGOR Pro (WaveMetrics, Portland, OR, USA). The transient responses in Ca^{2+} concentration within the first seconds after the stimulation were evaluated, with responses smaller than ± 5% of baseline values defined as non-responding cells. GABA-evoked responses showing Ca^{2+} transients with a decrease in amplitude lower than 5% from baseline were considered inhibitory and responses with an increase higher than 5% from baseline were defined as excitatory. Cells that showed both excitatory and inhibitory responses after one GABA stimulation were defined as biphasic. Per animal, two to three SCN slices were analyzed and the Ca^{2+} responses to GABA application were measured in 50 – 80 cells. For each animal we calculated the distribution of the different types of responses and the E/I ratio. To calculate the E/I ratio, we divided the number of cells that responded excitatory by the number of cells that responded inhibitory, per animal. Subsequently, we took the average of all the E/I ratios of all animals per group.

Statistical analysis was performed using SPSS (IBM, Armonk, NY, USA). We have used generalized estimating equations (GEE) to test if the average distribution of the GABA-induced responses (percentages of the 4 different types of responses) differs before and after treatment (ML077 or DMSO). We have used a multinomial regression model for the GEE and robust standard errors were calculated. We have used the number of cells per animal as a scale weight variable in the GEE to (extra) take into account the variability of the number of cells measured per SCN. Additional Wald tests shows whether the outcome of the GEE is significant. The effect of the treatment on the E/I ratio was tested with two-sided, paired t-tests, and the effect on baseline $[Ca^{2+}]_i$ was tested with the Mann-Whitney test, because these data did not pass the Shapiro-Wilk normality tests. Differences with $P \leq 0.05$ were considered significant.

3. Results/Discussion

Using Ca^{2+} imaging, we tested the effect of the recently developed KCC2 blocker ML077 on GABAergic responses in SCN cells. Previous studies have shown that Ca^{2+} transients are a reliable estimate of the neuronal activity, with elevations and reductions in $[Ca^{2+}]_i$ reflecting depolarization and hyperpolarization, respectively (Choi et al., 2008; Irwin and Allen, 2007; Irwin and Allen, 2009). GABAergic responses have been shown to be more excitatory during the night compared to the day (Choi et al., 2008; De Jeu and Pennartz, 2002), so we selected the mid-day for recordings to maximize the effect of ML077. Blocking KCC2 with ML077 caused an increase in excitatory responses after exogenous application of GABA (Fig 1 and Fig 2A; Wald chi2(1) = 23.61, $p = 1 \times 10^{-6}$, n = 8), leading to a change in E/I ratio from 0.95 to 3.41 (Fig 2B + 2C; t(7) = 3.45, p = 0.011, n = 8). To investigate which cells switched to the excitatory response type, we compared neurons before and after incubation with ML077. In 37% of all the cells, the type of the GABAergic response changed as a result of KCC2 blockage. Of the cells that initially responded to GABA in an inhibitory manner, 26% (n=55) became excitatory after incubation with ML077. About half of the inhibitory cells stayed inhibitory (n = 107; 51%) and the remaining inhibitory neurons became either biphasic (n = 14; 7%) or did not respond to GABA anymore (n = 35; 17%) Moreover, half of the neurons that initially did not respond to GABA (n = 48; 56%) and the majority of the biphasic responding neurons (n = 20; 69%) became excitatory as a result of ML077 application (Fig S1 + Fig 3A; Wald chi2(1) = 23.61, $p = 1 \times 10^{-6}$, n = 8). Since ML077 was dissolved in DMSO, we've used DMSO as control experiments. The control slices, incubated in ACSF containing the solvent DMSO (4 ppm), did not show alteration in the GABAergic response types (Fig S2 + Fig 3B; Wald chi2(1) = 1.40, p = 0.24, n = 4) nor did it show a shift in the E/I ratio (0.68 to 1.07, paired t-test; t(3) = 2.60, p = 0.08). Thus, the data demonstrate that the shift in E/I ratio is caused by inhibition of KCC2 by ML077.

We next performed Ca^{2+} imaging experiments with slices from animals entrained to long- and short days to determine whether KCC2 may play a role in photoperiod-induced changes in E/I ratio

reported previously (Farajnia et al., 2014). ML077 increased the percentage of cells showing excitatory responses in short photoperiod from 24% to 43%, which is equivalent to the fraction found after adaptation to long photoperiod conditions (Fig 4A1, 4B1 and (Farajnia et al., 2014)). Note that even in the presence of the KCC2 blocker, a difference in the E/I ratio between photoperiods still remains. This is in line with the observation that the percentage of excitatory cells increased to a similar degree in slices from mice adapted to long photoperiod and 12:12 condition, suggesting that KCC2 activity is important for maintaining E/I balance under all photoperiods. From all neurons that were initially inhibitory, about 50% stayed inhibitory, approximately 20-25% turned excitatory, and the remaining 25-30% became either non-responsive or responded in a biphasic manner. Moreover, about half of the non-responders and a significant part of the biphasic cells turned excitatory (Fig 3A and Fig 4A4; Wald chi2(1) = 36.62, $p = 1.44 \times 10^{-9}$+ 4B4; Wald chi2(1) = 5.52, p = 0.019). From all the slices measured, regardless of the photoperiod of the animal, the E/I ratio increased after blocking KCC2 (SP: Fig 4A2 + 4A3; t(7) = 3.92, p = 0.006, n = 8, and, LP: Fig 4B2 + 4B3; t(7) = 4.40, p = 0.003, n = 8). Together, these data show that, irrespective of their photoperiod, blocking KCC2 increases the amount of GABAergic excitation.

To determine if the drug influences the baseline $[Ca^{2+}]_i$, we analyzed the baseline $[Ca^{2+}]_i$ before and after application of either ML077 or DMSO. For all three photoperiods, we found an increase in baseline $[Ca^{2+}]_i$ after administration of ML077, which was not different to treatment with DMSO (Fig S3). Consequently, we can conclude that the rise in baseline $[Ca^{2+}]_i$ is not an effect of blocking KCC2 with ML077.

Furosemide and bumetanide are two pharmacological blockers that have been widely used to block the cotransporters KCC2 and NKCC1. Bumetanide has a higher affinity for NKCC1 than for KCC2 (Gillen et al., 1996; Payne et al., 2003), but furosemide is known to block both NKCC1 and KCC2 with equal potency (Blaesse et al., 2009; Delpire et al., 2009). Moreover, furosemide inhibits N-methyl D-aspartate (NMDA) and $GABA_A$ receptors (Staley, 2002). Blocking NKCC1 with bumetanide, and thus

the intrusion of Cl^-, does have an effect on the GABAergic response, but not on the polarity of the response. Bumetanide lowered the amplitude of GABA-evoked elevations in $[Ca^{2+}]_i$, but could not substantially convert GABAergic excitation into inhibition (Choi et al., 2008; Farajnia et al., 2014). A recent study by Klett and Allen (2017) demonstrated a larger effect on $[Cl^-]_i$ in SCN neurons due to application of the KCC2 blocker VU0240551 compared to bumetanide, suggesting a significant role of KCCs in the regulation of $[Cl^-]_i$. Our results show for the first time that a specific blocker for KCC2, ML077 (VU0255011), not only attenuates the GABAergic response in the SCN, but can even cause a reversal of the polarity of the GABAergic response from inhibition to excitation.

GABA is a dominant neurotransmitter in the SCN and has important roles in synchronization and entrainment (Albus et al., 2005). Modeling approaches and experimental evidence show that GABA signaling has significant impact on network function determining basic properties and plasticity of the SCN clock (Azzi et al., 2017; DeWoskin et al., 2015). Modulation of SCN network underlies encoding seasonal day-length changes with clustering of neuronal activity in short-days and wider phase distribution of the pacemaker cells in the SCN during long-days (VanderLeest et al., 2007). While there is still some controversy on the potential excitatory action of GABA in the adult SCN (see (Albers et al., 2017)), there is mounting evidence for excitatory GABA responses and the role of KCCs to regulate Cl^- concentration (Choi et al., 2008; Farajnia et al., 2014; Irwin and Allen, 2009; Myung et al., 2015). Functionally, the modulation of GABA response types and subsequent changes in E/I balance may affect SCN network plasticity. Our data show that just blocking KKC2 can already change the E/I balance in the SCN from a short-day to a long-day phenotype. Whether the changes in GABAergic E/I balance are sufficient or necessary for photoperiodic encoding by the SCN still needs to be established.

An imbalance between GABAergic excitation and inhibition is implicated in several neurological disorders (Marín, 2012; Sgadò et al., 2011) and because of its ability to reduce the level of GABAergic excitation, bumetanide is already used in several clinical trials for epilepsy and autism (Bruining et al.,

2015; Du et al., 2015; Eftekhari et al., 2013; Lemonnier et al., 2012; Pressler et al., 2015). Still, there is a demand for improved pharmacological blockers for the cotransporters, since the kinetics of bumetanide and furosemide are not optimal due to short half-life time and bad passage of the blood-brain barrier (Brandt et al., 2010). Our results already show the high effectiveness of ML077 for manipulating E/I balance in neuronal networks and this drug has been further optimized as VU0463271 (Delpire et al., 2012). Studies have shown that this new inhibitor leads to hippocampal hyperexcitability and seizure activity both in slices and in vivo (Kelley et al., 2016; Sivakumaran et al., 2015). These new and optimized KCC2 blockers are important tools for fundamental research on the role of chloride homeostasis in regulating E/I balance in neuronal networks.

While the mechanisms regulating and maintaining $[Cl^-]_i$ are still under debate, previous studies have shown a prominent role for CCCs (for review: (Ben-Ari, 2002; Payne et al., 2003)). Reduction or absence of KCC2 or its functionality leads to decreased inhibitory GABAergic actions (Deeb et al., 2011; Doyon et al., 2015; Hubner et al., 2001; Rivera et al., 1999; Zhu et al., 2005). Moreover, chloride dysregulation caused by reduced KCC2 expression or function is associated with numerous neurological disorders including epilepsy, chronic pain, and schizophrenia (Ben-Ari et al., 2012; Kelley et al., 2016; Miles et al., 2012; Price et al., 2005). Recently, Glykys et al. questioned the prominent role of KCC2 and NKCC1 by showing that blocking these cotransporters with VU0240551 and bumetanide did not change $[Cl^-]_i$, but that local intracellular and extracellular concentrations of anions determined $[Cl^-]_i$ (Glykys et al., 2014a). Since the argument on the role of immobile anions in $[Cl^-]_i$ regulation is not fully resolved yet (Glykys et al., 2014b; Luhmann et al., 2014; Voipio et al., 2014), this alternative or additional mechanism deserves further study. With our data, we show a significant increase in GABAergic excitation after blocking KCC2 with the new antagonist ML077. This GABA-mediated neuronal excitation presumably results from an increased $[Cl^-]_i$ and a correlated shift in GABA reversal potential. While impermeable anions may still contribute to the maintenance of $[Cl^-]_i$, our results support the hypothesis that cation-chloride-cotransporters play an important role in regulating the chloride homeostasis .

The question remains how photoperiod can affect chloride cotransporters to induce a change in E/I balance. Myung et al. recently demonstrated an increase in $[Cl^-]_i$ in the SCN cells after entrainment to long photoperiod. Moreover, application of furosemide to long photoperiod entrained SCN slices increased synchronization and lengthened the period of the circadian rhythms in *Bmal1*-Eluc in 12:12 entrained SCN explants to levels shown for the short photoperiod entrained SCN (Myung et al., 2015). Combined, these results suggest that modulation of the chloride levels in the cells can play a role in day-length encoding in the SCN. At the transcript level, the expression of both KCC2 and NKCC1 were upregulated in long photoperiod, when compared to short photoperiod, and the relative expression ratio between NKCC1 and KCC2 was significantly higher under long photoperiod in the dorsal SCN (Myung et al., 2015). Because these results only show the increase at mRNA level, one cannot conclude that NKCC1 causes the higher $[Cl^-]_i$ under long photoperiod. More important than mRNA or even protein expression is the functional expression and/or regulation of KCC2 vs NKCC1. The functionality of KCC2 is modulated by both transcriptional and post-transcriptional routes. (De)phosphorylation, recycling, and intracellular trafficking are, amongst others, examples of how KCC2 can be modulated and its function can be influenced (Kahle et al., 2013; Kahle and Delpire, 2016; Kaila et al., 2014; Lee et al., 2011; Mahadevan and Woodin, 2016). Therefore, the decrease in functional KCC2 and/or increase in functional NKCC1 in long photoperiod may contribute to elevated $[Cl^-]_i$ and consequently to the rise in GABAergic excitation. From our data we conclude that KCC2 plays an important role in the hyperpolarizing effect of GABA and thus in maintaining a low $[Cl^-]_i$. These data have potential societal impact as use of artificial light in modern society leads to “longer day length”. Moreover, GABAergic function is essential for sleep, anxiety, and depression. Whether day length also affects GABAergic function in other brain areas through this mechanism remains to be investigated.

Acknowledgements

We thank Dr. Craig Lindsley from the Vanderbilt University (Nashville, TN, USA) for providing us the first batch of ML077. We also thank Mayke Tersteeg for her technical assistance.

Funding

This work was supported by The Netherlands Organisation for Scientific Research/Netherlands Organisation for Health Research and Development Grant TOPGo 91210064 (to J.H.M.).

Fig. 1 SCN neurons can change GABAergic response after blocking KCC2 with ML077 (A) Examples of Fura-2-AM loaded SCN neurons from mice entrained to LD12:12. Color scale indicates fluorescence intensity at 380 nm excitation in arbitrary units. (Scale bar, 10 µm) (B) On top, a sketch of the experimental protocol is depicted. SCN slices were continuously superfused with ACSF and Ca^{2+} transients were recorded in response to focal applications of GABA (200 µM) given before and after a 10-minute incubation with ML077. Below example traces of Ca^{2+} transients of 4 neurons are shown demonstrating the changes in GABAergic response after blocking KCC2 with ML077. (Scale bars, 50 nM, 30 s)

Fig. 2 Blocking KCC2 with ML077 caused an increase in GABA-mediated excitation in SCN neurons of mice entrained to LD12:12. (A) Pie charts depicting the distributions of response types of the same SCN neurons on GABAergic stimulation before and after incubation with ML077 (number of cells: n = 499; measured in 23 slices of 8 animals). (B) Ratios of excitatory to inhibitory GABAergic signaling before and after incubation with ML077. Each value indicates the ratio of all the cells measured from one animal. (C) Increase in E/I ratio for each experiment after incubation with ML077 (B + C: (paired t-test; p = 0.011).

Fig. 3 GABAergic response type in SCN neurons (LD 12:12) changes after blocking KCC2 with ML077. (A) Distribution of GABAergic response types after incubation with ML077 grouped per initial GABAergic response type (number of cells per initial response type shown on the x-axis). The fraction of cells for each response type resulting from the ML077 treatment is depicted on the y-axis and shows a significant effect of the drug on response type distribution (total number of cells: n = 499; measured in 23 slices of 8 animals, Wald Chi square test; $p = 1 \times 10^{-6}$). (B) Distribution of GABAergic response types after incubation with control solution (4 ppm DMSO in ACSF) grouped per initial GABAergic response type (number of cells per initial response type shown on the x-axis). The fraction of

cells for each response type resulting from the DMSO treatment is depicted on the y-axis and shows no significant effect of the solvent (total number of cells: n = 248, measured in 11 slices of 4 animals, Wald Chi square test; p = 0.24).

Fig. 4 Changes in response type in SCN neurons after blocking KCC2 with ML077 is similar for all photoperiods. (A) Pie charts depicting the distributions of response types on GABAergic stimulation before and after incubation with ML077 (number of cells: n = 387; measured in 19 slices of 8 SCN) for SP entrained neurons. (B) Ratios of excitatory to inhibitory GABAergic signaling before and after incubation with ML077 for SP entrained neurons. Each value indicates the ratio of all the cells measured from one animal. (C) Increase in E/I ratio for each experiment after incubation with ML077 (B + C: (paired t-test; p = 0.006)). (D) Distribution of GABAergic response types after incubation with ML077 grouped per initial GABAergic response in SCN cells of mice entrained to SP (number of cells per initial response type shown on the x-axis). The fraction of cells for each response type resulting from the ML077 treatment is depicted on the y-axis and shows a significant effect of the drug on response type distribution (Wald Chi square test; $p = 1.44 \times 10^{-9}$). (E) Pie charts depicting the distributions of response types on GABAergic stimulation before and after incubation with ML077 (number of cells: n = 557; measured from 24 slices of 8 SCN) for LP entrained neurons. (F) Ratios of excitatory to inhibitory GABAergic signaling before and after incubation with ML077 for LP entrained neurons. Each value indicates the ratio of all the cells measured from one animal. (G) Increase in E/I ratio for each experiment after incubation with ML077 (F + G: (paired t-test; p = 0.003). (H) Distribution of GABAergic response types after incubation with ML077 grouped per initial GABAergic response in SCN cells of mice entrained to LP (number of cells per initial response type shown on the x-axis). The fraction of cells for each response type resulting from the ML077 treatment is depicted on the y-axis

and shows a significant effect of the drug on response type distribution (Wald Chi square test; p =0.019).

Fig S1 Changes in response type in SCN neurons after blocking KCC2 with ML077. Number of cells that change response type after incubation with ML077 grouped per initial GABAergic response in SCN cells of mice entrained to (A) LD12:12, (B) SP, and (C) LP. The number of cells for each response type resulting from the ML077 treatment is depicted on the y-axis and shows a significant effect of the drug on response type distribution (number of cells per initial response type shown on the x-axis) (LD12:12: Wald Chi square test; $p = 1 \times 10^{-6}$ SP: Wald Chi square test; $p = 1.44 \times 10^{-9}$ LP: Wald Chi square test; p =0.019).

Fig S2 DMSO treatment does not affect GABAergic responses. On top, a sketch of the experimental protocol is depicted. SCN slices were continuously superfused with ACSF and Ca^{2+} transients were recorded in response to focal applications of GABA (200 µM) given before and after a 10-minute incubation with DMSO in ACSF (4ppm). Below example traces of Ca^{2+} transients of 5 neurons are shown demonstrating the GABAergic responses before and after incubation with control solution (4 ppm DMSO in ACSF). (Scale bars, 50 nM, 30 s)

Fig. S3 Rise in baseline $[Ca^{2+}]_i$ is not an effect of blocking KCC2 with ML077. Bar graphs show average increase (means ± SEM) in baseline $[Ca^{2+}]_i$ after application of ML077 and DMSO from all cells of animals entrained to LD12:12 (Mann-Whitney test: p = 0.069, ML077: n = 499, DMSO: n = 269), SP (Mann-Whitney test: p = 0.0141, ML077: n = 387, DMSO: n = 149), and LP (Mann-Whitney test: p = 0.153, ML077: n = 557, DMSO: n = 319).

Figure 1

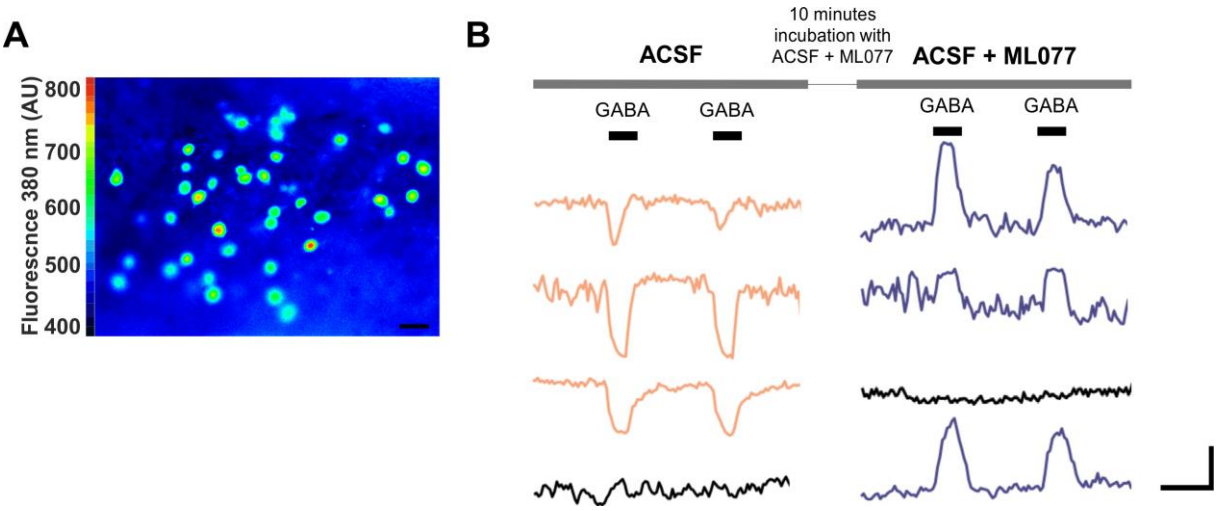

Figure 2

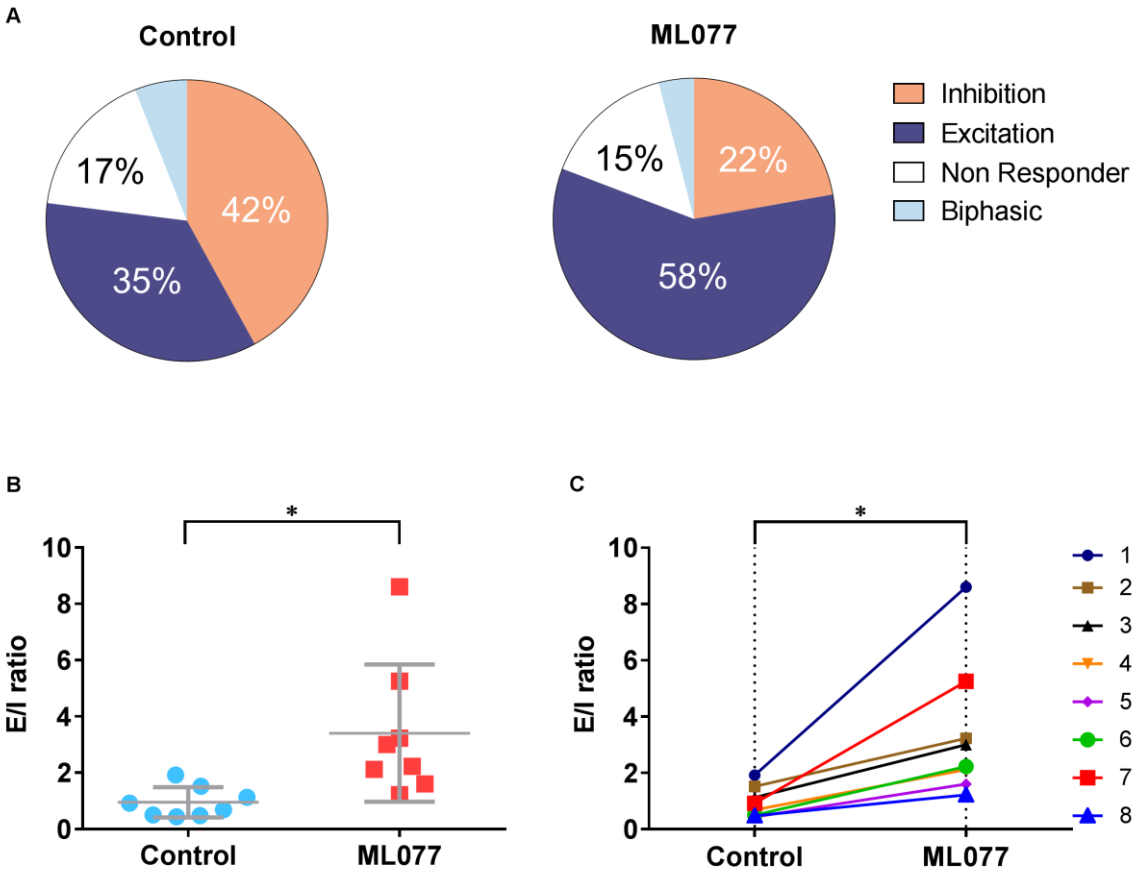

Figure 3

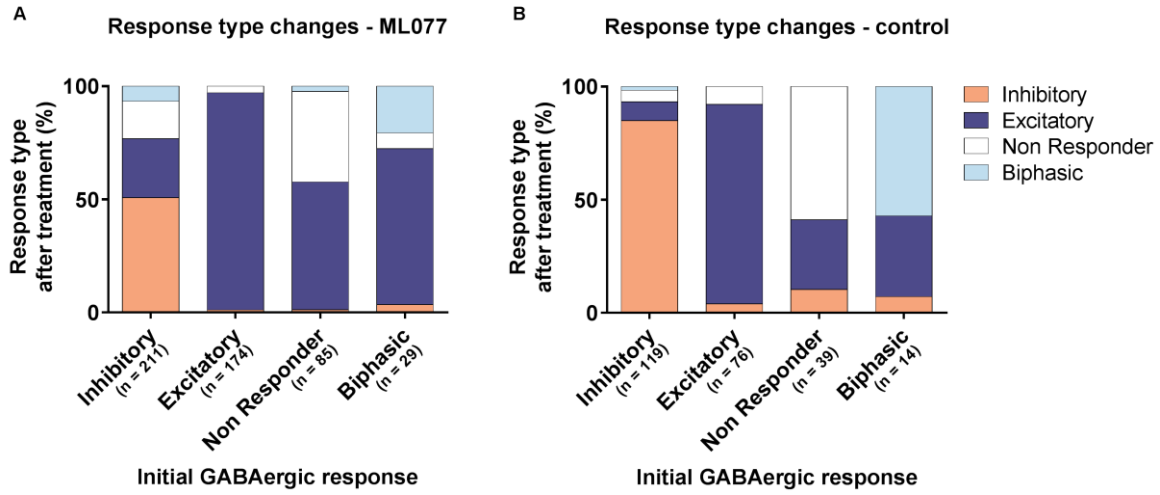
A
Response type changes - ML077
Response type after treatment (%)
100
50
0
Inhibitory (n = 211)
Excitatory (n = 174)
Non Responder (n = 85)
Biphasic (n = 29)
Initial GABAergic response
B
Response type changes - control
Response type after treatment (%)
100
50
0
Inhibitory (n = 119)
Excitatory (n = 76)
Non Responder (n = 39)
Biphasic (n = 14)
Initial GABAergic response
Inhibitory
Excitatory
Non Responder
Biphasic

Figure 4

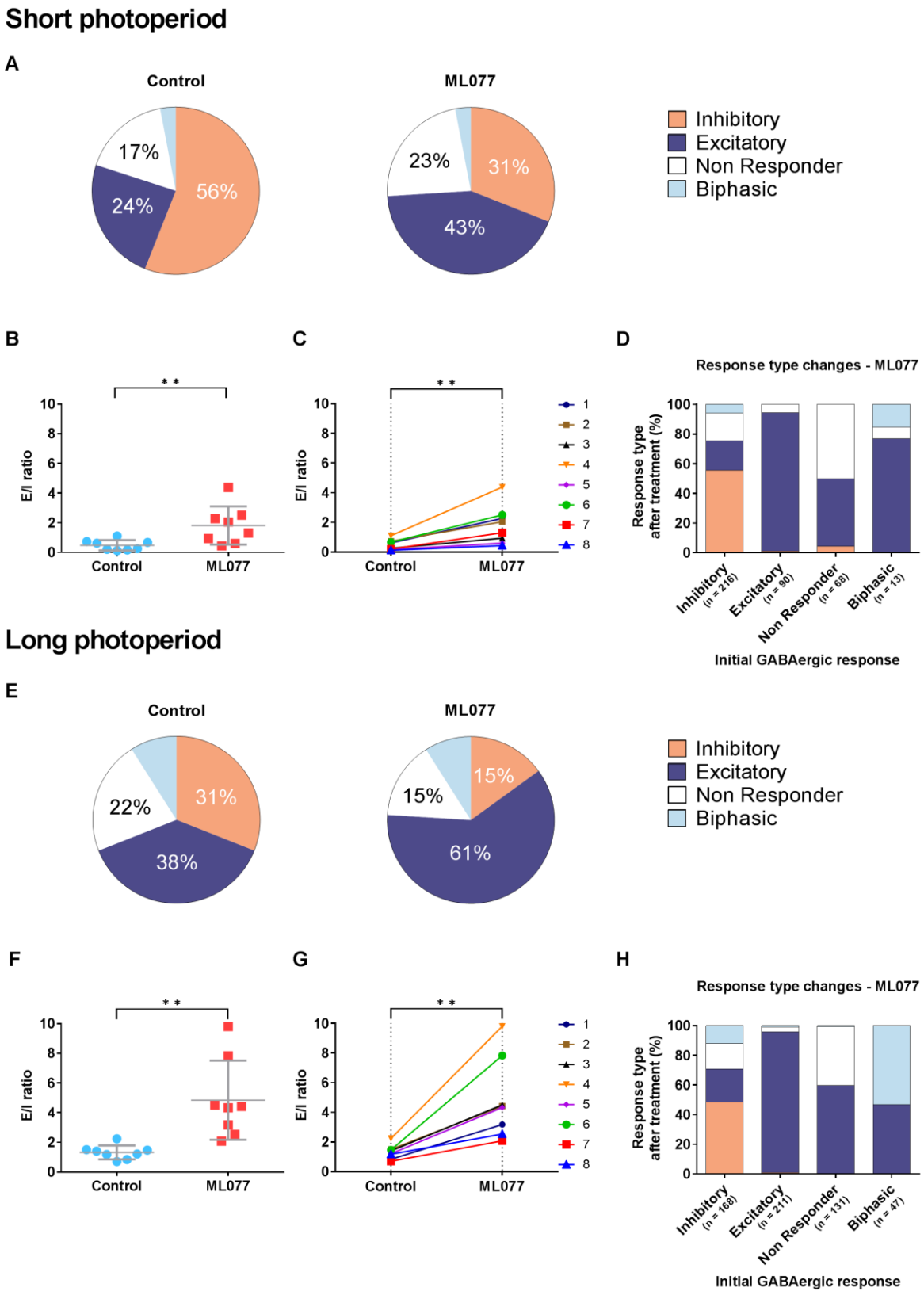
Short photoperiod
A
Control
ML077
17%
56%
24%
23%
31%
43%
Inhibitory
Excitatory
Non Responder
Biphasic
B
C
D
E/I ratio
Control
ML077
Response type changes - ML077
Response type after treatment (%)
Inhibitory (n = 216)
Excitatory (n = 90)
Non Responder (n = 68)
Biphasic (n = 13)
Initial GABAergic response
Long photoperiod
E
22%
31%
38%
15%
15%
61%
F
G
H
Inhibitory (n = 168)
Excitatory (n = 211)
Non Responder (n = 131)
Biphasic (n = 47)

Figure S1

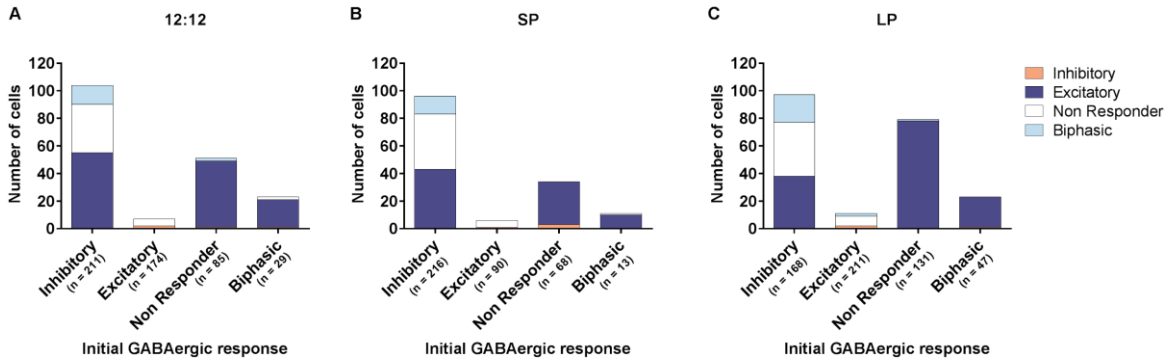

Figure S2

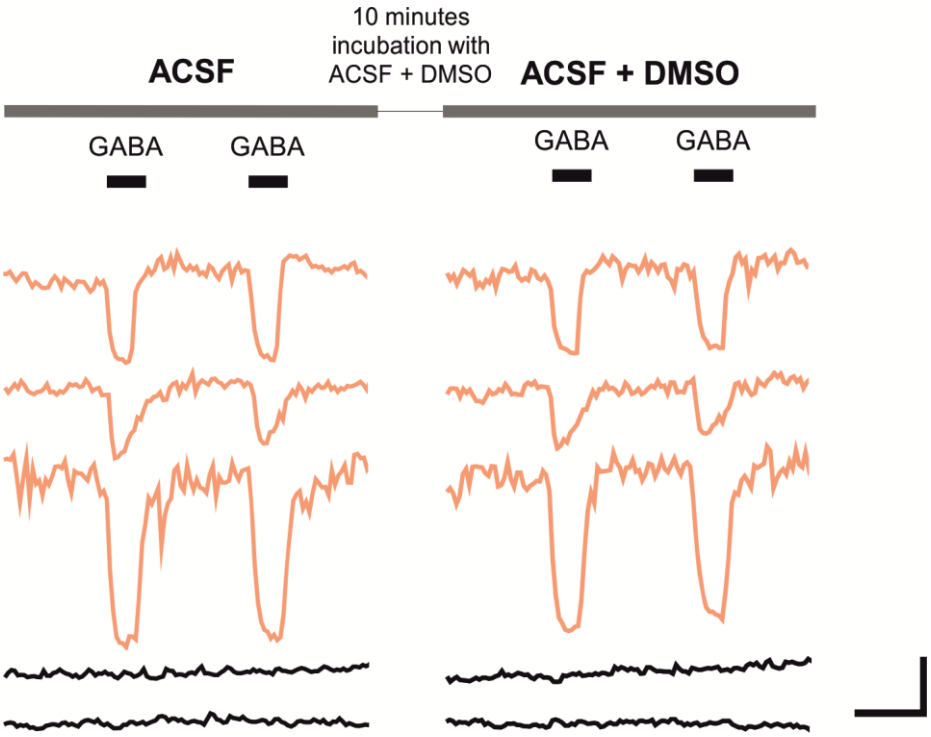

Figure S3

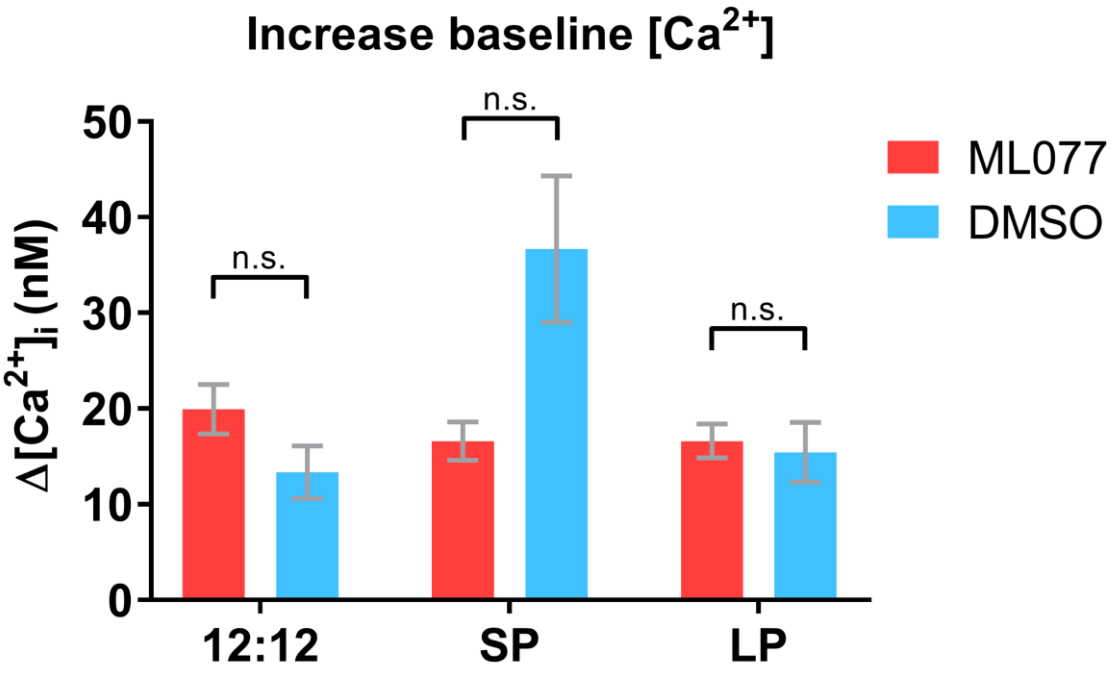
Increase baseline [Ca2+]
Δ[Ca2+]i (nM)
50
40
30
20
10
0
n.s.
n.s.
n.s.
12:12
SP
LP
ML077
DMSO

References

Albers, H. E., Walton, J. C., Gamble, K. L., McNeill, J. K. t., Hummer, D. L., 2017. The dynamics of GABA signaling: Revelations from the circadian pacemaker in the suprachiasmatic nucleus. Front Neuroendocrinol 44, 35-82.

Albus, H., Vansteensel, M. J., Michel, S., Block, G. D., Meijer, J. H., 2005. A GABAergic mechanism is necessary for coupling dissociable ventral and dorsal regional oscillators within the circadian clock. Current biology : CB 15, 886-893.

Azzi, A., Evans, J. A., Leise, T., Myung, J., Takumi, T., Davidson, A. J., Brown, S. A., 2017. Network Dynamics Mediate Circadian Clock Plasticity. Neuron 93, 441-450.

Ben-Ari, Y., 2002. Excitatory actions of gaba during development: the nature of the nurture. Nature reviews. Neuroscience 3, 728-739.

Ben-Ari, Y., Khalilov, I., Kahle, K. T., Cherubini, E., 2012. The GABA excitatory/inhibitory shift in brain maturation and neurological disorders. Neuroscientist 18, 467-486.

Blaesse, P., Airaksinen, M. S., Rivera, C., Kaila, K., 2009. Cation-chloride cotransporters and neuronal function. Neuron 61, 820-838.

Brandt, C., Nozadze, M., Heuchert, N., Rattka, M., Loscher, W., 2010. Disease-modifying effects of phenobarbital and the NKCC1 inhibitor bumetanide in the pilocarpine model of temporal lobe epilepsy. J Neurosci 30, 8602-8612.

Bruining, H., Passtoors, L., Goriounova, N., Jansen, F., Hakvoort, B., de Jonge, M., Poil, S. S., 2015. Paradoxical Benzodiazepine Response: A Rationale for Bumetanide in Neurodevelopmental Disorders? Pediatrics 136, e539-543.

Buzsaki, G., Kaila, K., Raichle, M., 2007. Inhibition and brain work. Neuron 56, 771-783.

Choi, H. J., Lee, C. J., Schroeder, A., Kim, Y. S., Jung, S. H., Kim, J. S., Kim, D. Y., Son, E. J., Han, H. C., Hong, S. K., Colwell, C. S., Kim, Y. I., 2008. Excitatory actions of GABA in the suprachiasmatic nucleus. The Journal of neuroscience : the official journal of the Society for Neuroscience 28, 5450-5459.

Chung, L., 2012. Recent progress in GABAergic excitation from mature brain. Archives of pharmacal research 35, 2035-2044.

Costa, E., 1998. From GABAA receptor diversity emerges a unified vision of GABAergic inhibition. Annu Rev Pharmacol Toxicol 38, 321-350.

De Jeu, M., Pennartz, C., 2002. Circadian modulation of GABA function in the rat suprachiasmatic nucleus: excitatory effects during the night phase. J Neurophysiol 87, 834-844.

Deeb, T. Z., Lee, H. H. C., Walker, J. A., Davies, P. A., Moss, S. J., 2011. Hyperpolarizing GABAergic transmission depends on KCC2 function and membrane potential. Channels (Austin, Tex.) 5, 475-481.

Delpire, E., Baranczak, A., Waterson, A. G., Kim, K., Kett, N., Morrison, R. D., Daniels, J. S., Weaver, C. D., Lindsley, C. W., 2012. Further optimization of the K-Cl cotransporter KCC2 antagonist ML077: development of a highly selective and more potent in vitro probe. Bioorg Med Chem Lett 22, 4532-4535.

Delpire, E., Days, E., Lewis, L. M., Mi, D., Kim, K., Lindsley, C. W., Weaver, C. D., 2009. Small-molecule screen identifies inhibitors of the neuronal K-Cl cotransporter KCC2. Proc Natl Acad Sci U S A 106, 5383-5388.

DeWoskin, D., Myung, J., Belle, M. D., Piggins, H. D., Takumi, T., Forger, D. B., 2015. Distinct roles for GABA across multiple timescales in mammalian circadian timekeeping. Proc Natl Acad Sci U S A 112, E3911-3919.

Doyon, N., Prescott, S. A., De Koninck, Y., 2015. Mild KCC2 Hypofunction Causes Inconspicuous Chloride Dysregulation that Degrades Neural Coding. Front Cell Neurosci 9, 516.

Du, L., Shan, L., Wang, B., Li, H., Xu, Z., Staal, W. G., Jia, F., 2015. A Pilot Study on the Combination of Applied Behavior Analysis and Bumetanide Treatment for Children with Autism. J Child Adolesc Psychopharmacol 25, 585-588.
Eftekhari, S., Mehvari Habibabadi, J., Najafi Ziarani, M., Hashemi Fesharaki, S. S., Gharakhani, M., Mostafavi, H., Joghataei, M. T., Beladimoghadam, N., Rahimian, E., Hadjighassem, M. R., 2013. Bumetanide reduces seizure frequency in patients with temporal lobe epilepsy. Epilepsia 54, e9-12.
Farajnia, S., van Westering, T. L. E., Meijer, J. H., Michel, S., 2014. Seasonal induction of GABAergic excitation in the central mammalian clock. Proceedings of the National Academy of Sciences of the United States of America 111, 9627-9632.
Gamba, G., 2005. Molecular physiology and pathophysiology of electroneutral cation-chloride cotransporters. Physiological reviews 85, 423-493.
Gillen, C. M., Brill, S., Payne, J. A., Forbush, B., 3rd, 1996. Molecular cloning and functional expression of the K-Cl cotransporter from rabbit, rat, and human. A new member of the cation-chloride cotransporter family. J Biol Chem 271, 16237-16244.
Glykys, J., Dzhala, V., Egawa, K., Balena, T., Saponjian, Y., Kuchibhotla, K. V., Bacskai, B. J., Kahle, K. T., Zeuthen, T., Staley, K. J., 2014a. Local impermeant anions establish the neuronal chloride concentration. Science (New York, N.Y.) 343, 670-675.
Glykys, J., Dzhala, V., Egawa, K., Balena, T., Saponjian, Y., Kuchibhotla, K. V., Bacskai, B. J., Kahle, K. T., Zeuthen, T., Staley, K. J., 2014b. Response to comments on "Local impermeant anions establish the neuronal chloride concentration". Science (New York, N.Y.) 345, 1130.
Haider, B., Duque, A., Hasenstaub, A. R., McCormick, D. A., 2006. Neocortical network activity in vivo is generated through a dynamic balance of excitation and inhibition. J Neurosci 26, 4535-4545.
Hubner, C. A., Stein, V., Hermans-Borgmeyer, I., Meyer, T., Ballanyi, K., Jentsch, T. J., 2001. Disruption of KCC2 reveals an essential role of K-Cl cotransport already in early synaptic inhibition. Neuron 30, 515-524.
Irwin, R. P., Allen, C. N., 2007. Calcium response to retinohypothalamic tract synaptic transmission in suprachiasmatic nucleus neurons. J Neurosci 27, 11748-11757.
Irwin, R. P., Allen, C. N., 2009. GABAergic signaling induces divergent neuronal Ca2+ responses in the suprachiasmatic nucleus network. The European journal of neuroscience 30, 1462-1475.
Kahle, K. T., Deeb, T. Z., Puskarjov, M., Silayeva, L., Liang, B., Kaila, K., Moss, S. J., 2013. Modulation of neuronal activity by phosphorylation of the K-Cl cotransporter KCC2. Trends Neurosci 36, 726-737.
Kahle, K. T., Delpire, E., 2016. Kinase-KCC2 coupling: Cl- rheostasis, disease susceptibility, therapeutic target. J Neurophysiol 115, 8-18.
Kaila, K., 1994. Ionic basis of GABAA receptor channel function in the nervous system. Prog Neurobiol 42, 489-537.
Kaila, K., Price, T. J., Payne, J. A., Puskarjov, M., Voipio, J., 2014. Cation-chloride cotransporters in neuronal development, plasticity and disease. Nat Rev Neurosci 15, 637-654.
Kelley, M. R., Deeb, T. Z., Brandon, N. J., Dunlop, J., Davies, P. A., Moss, S. J., 2016. Compromising KCC2 transporter activity enhances the development of continuous seizure activity. Neuropharmacology 108, 103-110.
Klett, N. J., Allen, C. N., 2017. Intracellular Chloride Regulation in AVP+ and VIP+ Neurons of the Suprachiasmatic Nucleus. Sci Rep 7, 10226.

Lee, H. H. C., Deeb, T. Z., Walker, J. A., Davies, P. A., Moss, S. J., 2011. NMDA receptor activity downregulates KCC2 resulting in depolarizing GABAA receptor-mediated currents. Nature neuroscience 14, 736-743.
Lemonnier, E., Degrez, C., Phelep, M., Tyzio, R., Josse, F., Grandgeorge, M., Hadjikhani, N., Ben-Ari, Y., 2012. A randomised controlled trial of bumetanide in the treatment of autism in children. Transl Psychiatry 2, e202.
Lindsley, C., Lewis, M., Weaver, D., Delpire, E., 2010. Discovery of a Highly Selective KCC2 Antagonist. Probe Reports from the NIH Molecular Libraries Program. National Center for Biotechnology Information (US), Bethesda (MD).
Luhmann, H. J., Kirischuk, S., Kilb, W., 2014. Comment on "Local impermeant anions establish the neuronal chloride concentration". Science (New York, N.Y.) 345, 1130.
Macdonald, R. L., Olsen, R. W., 1994. GABAA receptor channels. Annu Rev Neurosci 17, 569-602.
Mahadevan, V., Woodin, M. A., 2016. Regulation of neuronal chloride homeostasis by neuromodulators. J Physiol 594, 2593-2605.
Marín, O., 2012. Interneuron dysfunction in psychiatric disorders. Nature reviews. Neuroscience 13, 107-120.
Michel, S., Marek, R., Vanderleest, H. T., Vansteensel, M. J., Schwartz, W. J., Colwell, C. S., Meijer, J. H., 2013. Mechanism of bilateral communication in the suprachiasmatic nucleus. The European journal of neuroscience 37, 964-971.
Miles, R., Blaesse, P., Huberfeld, G., Wittner, L., Kaila, K., 2012. Chloride homeostasis and GABA signaling in temporal lobe epilepsy. Jasper's Basic Mechanisms of the Epilepsies.
Myung, J., Hong, S., DeWoskin, D., De Schutter, E., Forger, D. B., Takumi, T., 2015. GABA-mediated repulsive coupling between circadian clock neurons in the SCN encodes seasonal time. Proc Natl Acad Sci U S A 112, E3920-3929.
Nelson, S. B., Valakh, V., 2015. Excitatory/Inhibitory Balance and Circuit Homeostasis in Autism Spectrum Disorders. Neuron 87, 684-698.
Payne, J. A., Rivera, C., Voipio, J., Kaila, K., 2003. Cation-chloride co-transporters in neuronal communication, development and trauma. Trends Neurosci 26, 199-206.
Pressler, R. M., Boylan, G. B., Marlow, N., Blennow, M., Chiron, C., Cross, J. H., de Vries, L. S., Hallberg, B., Hellstrom-Westas, L., Jullien, V., Livingstone, V., Mangum, B., Murphy, B., Murray, D., Pons, G., Rennie, J., Swarte, R., Toet, M. C., Vanhatalo, S., Zohar, S., 2015. Bumetanide for the treatment of seizures in newborn babies with hypoxic ischaemic encephalopathy (NEMO): an open-label, dose finding, and feasibility phase 1/2 trial. Lancet Neurol 14, 469-477.
Price, T. J., Cervero, F., de Koninck, Y., 2005. Role of cation-chloride-cotransporters (CCC) in pain and hyperalgesia. Curr Top Med Chem 5, 547-555.
Rivera, C., Voipio, J., Payne, J. A., Ruusuvuori, E., Lahtinen, H., Lamsa, K., Pirvola, U., Saarma, M., Kaila, K., 1999. The K+/Cl- co-transporter KCC2 renders GABA hyperpolarizing during neuronal maturation. Nature 397, 251-255.
Sgadò, P., Dunleavy, M., Genovesi, S., Provenzano, G., Bozzi, Y., 2011. The role of GABAergic system in neurodevelopmental disorders: a focus on autism and epilepsy. International journal of physiology, pathophysiology and pharmacology 3, 223-235.
Sivakumaran, S., Cardarelli, R. A., Maguire, J., Kelley, M. R., Silayeva, L., Morrow, D. H., Mukherjee, J., Moore, Y. E., Mather, R. J., Duggan, M. E., Brandon, N. J., Dunlop, J., Zicha, S., Moss, S. J., Deeb, T. Z., 2015. Selective inhibition of KCC2 leads to hyperexcitability and epileptiform discharges in hippocampal slices and in vivo. J Neurosci 35, 8291-8296.
Sivilotti, L., Nistri, A., 1991. GABA receptor mechanisms in the central nervous system. Prog Neurobiol 36, 35-92.

Staley, K. J., 2002. Diuretics as Antiepileptic Drugs: Should We Go with the Flow? Epilepsy Curr 2, 35-38.
VanderLeest, H. T., Houben, T., Michel, S., Deboer, T., Albus, H., Vansteensel, M. J., Block, G. D., Meijer, J. H., 2007. Seasonal encoding by the circadian pacemaker of the SCN. Current biology : CB 17, 468-473.
Voipio, J., Boron, W. F., Jones, S. W., Hopfer, U., Payne, J. A., Kaila, K., 2014. Comment on "Local impermeant anions establish the neuronal chloride concentration". Science 345, 1130.
Wagner, S., Castel, M., Gainer, H., Yarom, Y., 1997. GABA in the mammalian suprachiasmatic nucleus and its role in diurnal rhythmicity. Nature 387, 598-603.
Zhu, L., Lovinger, D., Delpire, E., 2005. Cortical neurons lacking KCC2 expression show impaired regulation of intracellular chloride. J Neurophysiol 93, 1557-1568.